

Supplementary information to **eIF4B stimulates eIF4A ATPase and unwinding activities by direct interaction through its 7-repeats region**, Alexandra Z. Andreou, Ulf Harms & Dagmar Klostermeier.

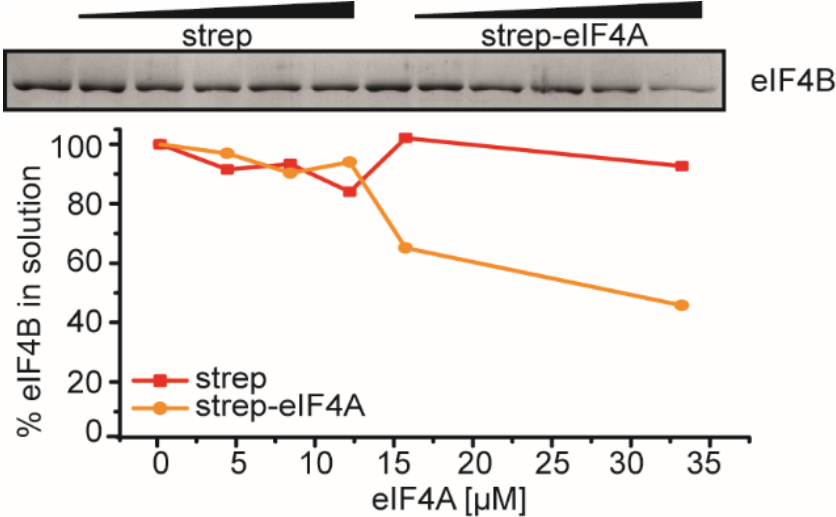
## Supplementary Table

Table S1: **Oligonucleotides used in this study**

| #      | primer                   | sequence (5'→3')                             |
|--------|--------------------------|--|
| PB-001 | <i>Tif3</i> _ΔNTD-FW     | CCACCATATGTCGGATAGAAGAGAGGAATACCC            |
| PB-002 | <i>Tif3</i> _ΔCTD-N      | CAGTTTGGTAAGTAACCTCAAC                       |
| PB-003 | <i>Tif3</i> _ΔCTD-C      | GTTGAGGTTACTTACCAAACCTG                      |
| PB-004 | <i>Tif3</i> _ΔRRM-N      | GCACCTCCCCCTCTTCTTGGAGGGTATTCCTCTCTTCTATCGGA |
| PB-005 | <i>Tif3</i> _ΔRRM-C      | CCAAGAAGAGGGGGAGGTGC                         |
| PB-006 | <i>Tif3</i> _ΔNTDΔRRM-FW | CCACCATATGCCAAGAAGAGGGGGAGGTGCAGAT           |
| PB-007 | <i>Tif3</i> _Δr1-7-FW    | GGTATTTTTGGTTTGTGAGGAGCCGCAACAGAACTGAAAC     |
| PB-008 | <i>Tif3</i> _Δr1-7-RV    | CCTCAACAAACCAAAAATA                          |
| PB-009 | <i>Tif3</i> _r1-7-FW     | GTAG CCACCATATGCCAAGAAGAGGG                  |
| PB-010 | <i>Tif3</i> _r1-7-RV     | GTCAGCGGATCCTTATTACTTACCAAACCTG              |
| PB-011 | <i>Tif3</i> -FW          | GGCATATGATGGCTCCACCAAAGAAAACCG               |
| PB-012 | <i>Tif3</i> -RV          | CGGATCCCTATTTCTTACCAACAACCTTCCC              |
| PB-013 | <i>Tif3</i> -CFW         | CCAAGGCTCTTGCAGACCACC                        |
| PB-014 | <i>Tif3</i> -CRV         | GGTGGTCTGCAAGAGCCTTGG                        |

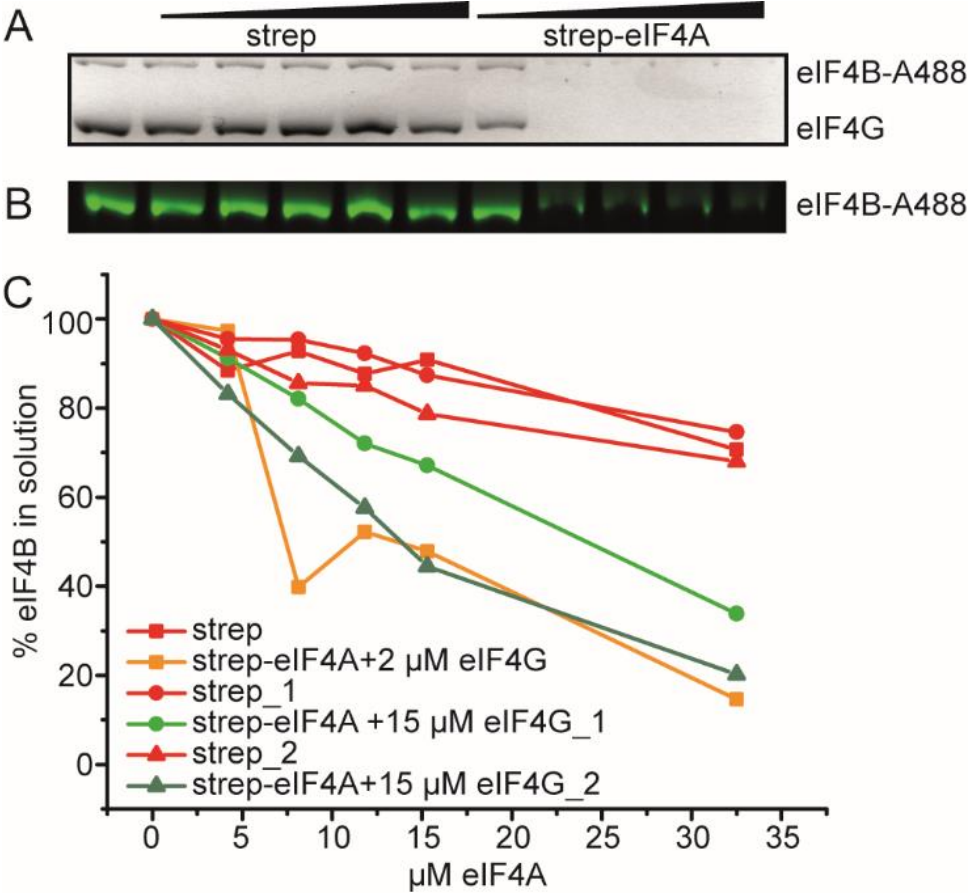
Supplementary Figures

Figure S1: eIF4B binds to eIF4A in the presence of ADPNP and RNA.



Supernatant depletion assay to follow binding of 0.5 μM eIF4B to eIF4A-bio in the presence of 5 μM RNA (32mer) and 10 mM ADPNP (Coomassie Blue staining). eIF4A-bio concentrations are 0, 4, 8, 12, 15 and 33 μM. eIF4B in the supernatant was quantified by densitometry. Red: depletion upon addition of streptavidin beads (negative control), yellow: depletion upon addition of eIF4A-conjugated streptavidin beads.

Figure S2: eIF4B binding to eIF4A is not affected by eIF4G.

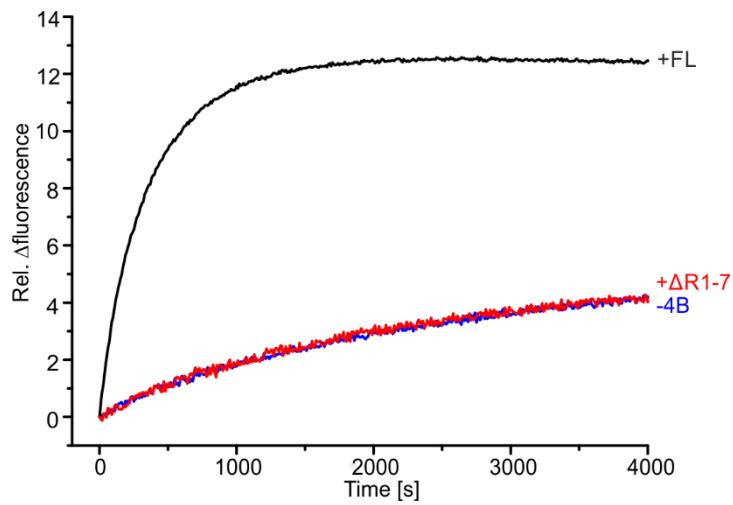


**A:** Supernatant depletion assay to follow binding of 0.25 μM eIF4B-A488 to eIF4A-bio in the presence of 10 mM ADPNP, 5 μM RNA (32mer) and 2 μM eIF4G (Coomassie Blue staining)

**B:** Same as in panel A, but with fluorescence detection.

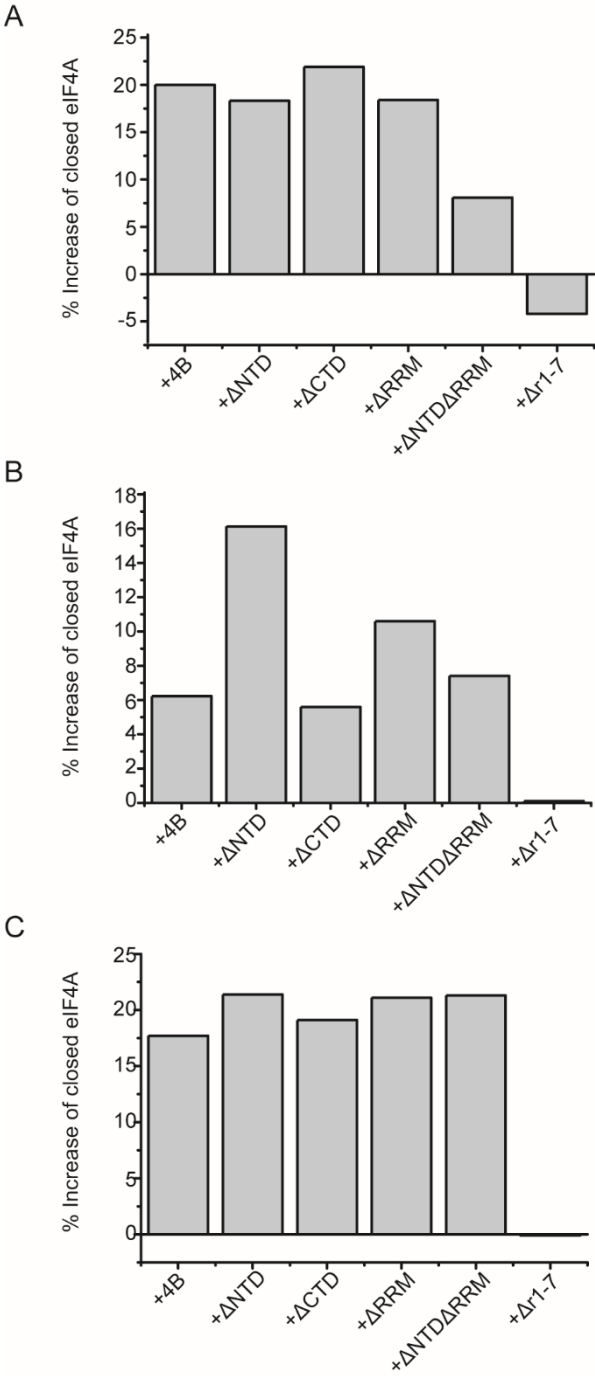
**C:** Quantification of the amount of eIF4B in the supernatant by fluorescence detection upon addition of streptavidin beads (red) or eIF4A-conjugated streptavidin beads in the presence of 2 μM (orange) or 15 μM eIF4G (light/dark green, two independent experiments).

Figure S3: RNA unwinding by eIF4A in the presence of DNA trap.



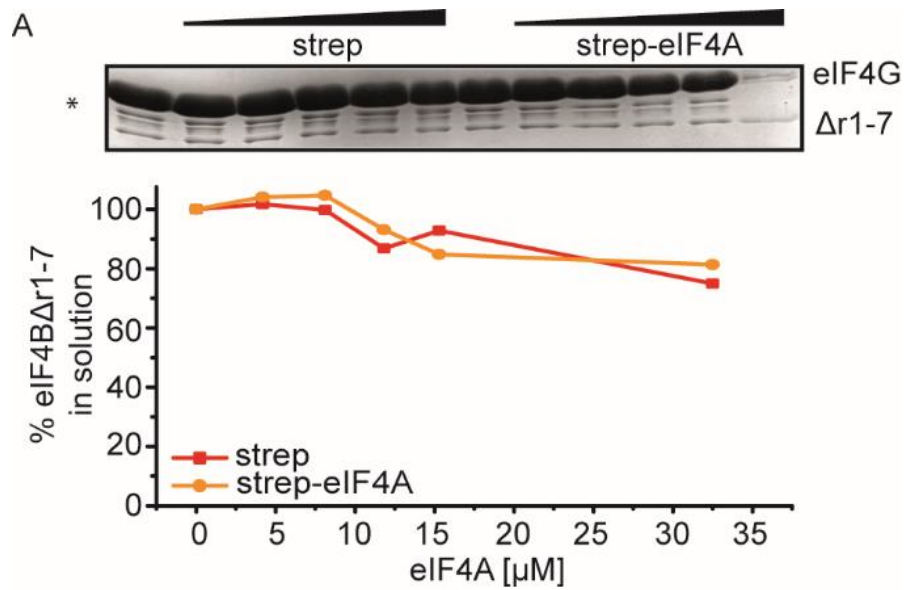
32mer/9mer RNA unwinding by eIF4A in the presence of eIF4G (blue), eIF4G and eIF4B (black) or eIF4G and eIF4B\_Δr1-7 (red), followed by a decrease in FRET (i.e. decrease in Cy5 fluorescence, plotted here as an increase). The 9mer RNA strand released upon unwinding was trapped by a 9mer DNA oligonucleotide (5'-AGGTCCCAA-3'). Rate constants for unwinding are  $k_{\text{unwind}} = 0.42 \cdot 10^{-3} \text{ s}^{-1}$  (eIF4A/eIF4G),  $k_{\text{unwind}} = 2.67 \cdot 10^{-3} \text{ s}^{-1}$  (eIF4A/eIF4G/eIF4B) and  $k_{\text{unwind}} = 0.47 \cdot 10^{-3} \text{ s}^{-1}$  (eIF4A/eIF4G/eIF4B\_Δr1-7).

Figure S4: eIF4B\_Δr1-7 fails to stimulate the eIF4A conformational change to the closed state.



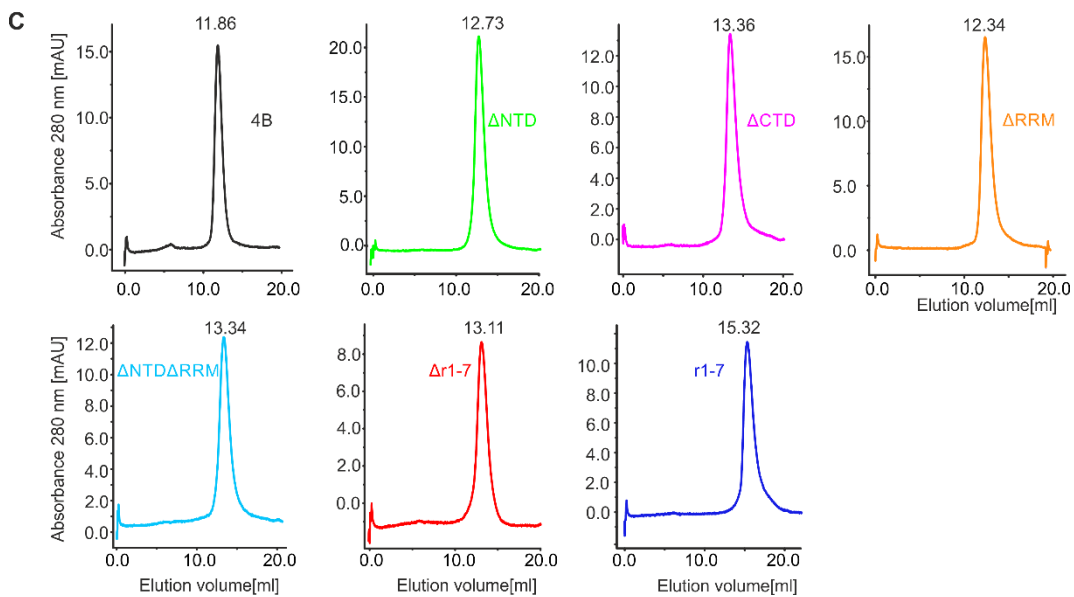
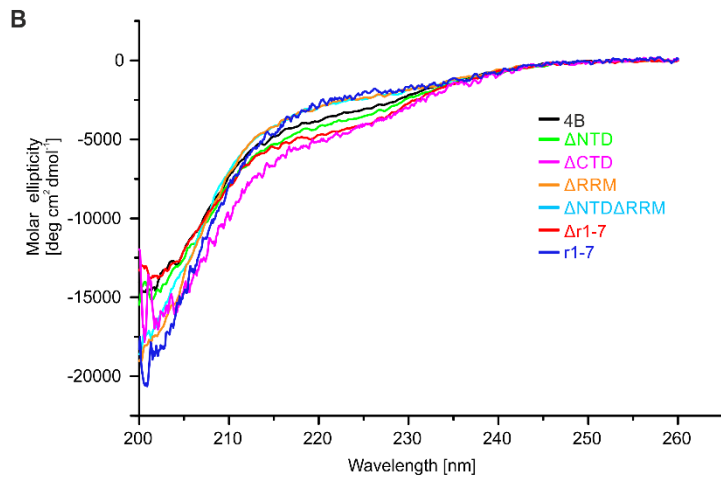
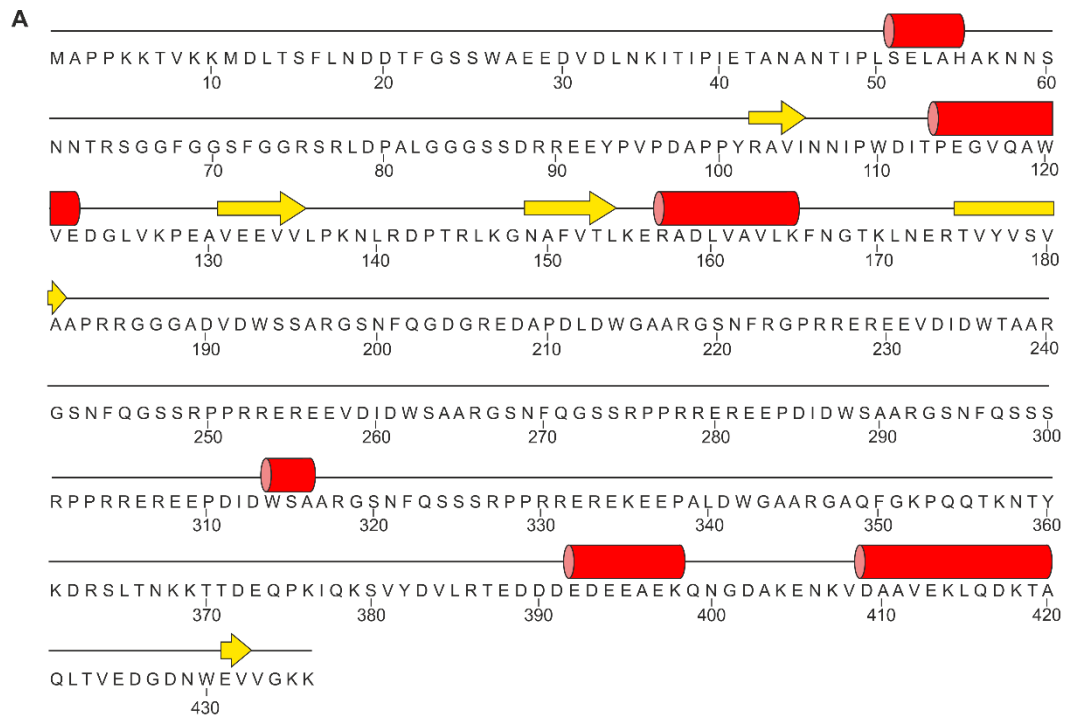
Increase of the population of eIF4A in the closed state upon addition of wild-type eIF4B and deletion variants. The three panels A, B, and C show the results from three independent experiments, performed with different batches of labeled eIF4A on different days. eIF4B lacking the 7-repeats region (eIF4B\_Δr1-7) does not promote the eIF4A conformational change.

Figure S5: eIF4G does not promote binding of eIF4B\_Δr1-7 to eIF4A.



Supernatant depletion assay with eIF4A-bio and 0.5 μM of eIF4B\_Δr1-7 in the presence of 5 μM 32mer RNA, 15 μM eIF4G and 10 mM ADPNP (Coomassie Blue staining). eIF4B\_Δr1-7 in the supernatant was quantified by densitometry. Red: depletion upon addition of streptavidin beads (negative control), yellow: depletion upon addition of eIF4A-conjugated streptavidin beads. The bands between the band for eIF4G and eIF4B\_Δr1-7 are eIF4G degradation products.

Figure S6: Analysis of folding of eIF4B variants.



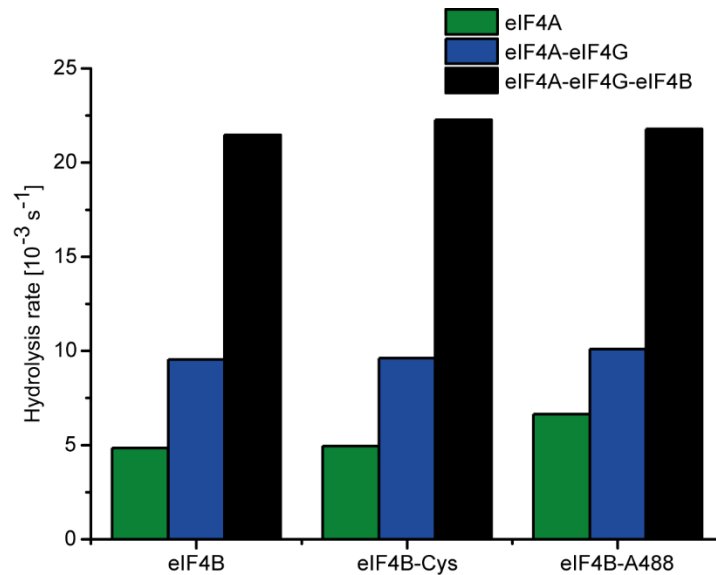
**A:** Prediction of secondary structure elements of eIF4B using PSIPRED {Jones, 1999 #3765}.  $\beta$ -strands are indicated by arrows,  $\alpha$ -helical regions are depicted by cylinders.

**B:** Far-UV CD spectra of eIF4B variants. Measurements were performed with a protein concentration of 0.25 mg/ml in 10 mM HEPES/KOH, pH 7.5, 100 mM NaCl at 25 °C.

**C:** Elution profiles of eIF4B variants from an analytical Superdex 200 (10/300) chromatography column, equilibrated with 50 mM Tris/HCl, pH 7.5, 100 mM NaCl. Size-exclusion chromatography was performed with 250  $\mu$ l of a  $\sim$ 3  $\mu$ M solution of protein at room temperature with a flow rate of 0.7 ml  $\text{min}^{-1}$ .



Figure S7: Fluorescently labeled eIF4B stimulates eIF4A ATPase activity



eIF4B, eIF4B<sub>248C/274C</sub> (eIF4B-Cys) and Alexa488-labeled eIF4B<sub>248C/274C</sub> (eIF4B<sub>A488</sub>) stimulate the RNA-dependent ATPase activity of eIF4A to the same extent. Experiments were performed in presence of 25  $\mu\text{M}$  poly(U) RNA. In the absence of additional factors, eIF4A hydrolyzes ATP with  $k_{\text{cat}} = 4.9 \cdot 10^{-3} \text{ s}^{-1}$ ,  $k_{\text{cat}} = 4.9 \cdot 10^{-3} \text{ s}^{-1}$  and  $k_{\text{cat}} = 6.6 \cdot 10^{-3} \text{ s}^{-1}$  (green) In the presence of eIF4G, the rates were  $k_{\text{cat}} = 9.6 \cdot 10^{-3} \text{ s}^{-1}$ ,  $k_{\text{cat}} = 9.6 \cdot 10^{-3} \text{ s}^{-1}$ , and  $k_{\text{cat}} = 10.1 \cdot 10^{-3} \text{ s}^{-1}$ , respectively (blue). After addition of eIF4B, eIF4B-Cys or eIF4B-A488,  $k_{\text{cat}}$  values were increased to  $21.5 \cdot 10^{-3} \text{ s}^{-1}$ ,  $22.3 \cdot 10^{-3} \text{ s}^{-1}$  and  $21.8 \cdot 10^{-3} \text{ s}^{-1}$ , respectively (black).